Remote Sensing of Environment

Supporting Information for

Fossil fuel CO2 emissions over metropolitan areas from space: a multi-model analysis of OCO-2 data over Lahore, Pakistan

Ruixue Lei [1], Sha Feng [1,2], Alexandre Danjou [3], Grégoire Broquet [3], Dien Wu [4], John C. Lin [5], Christopher W. O'Dell [6], Thomas Lauvaux [1,3]

[1] Department of Meteorology and Atmospheric Science, The Pennsylvania State University, University Park, PA, USA

[2] Atmospheric Sciences and Global Change Division, Pacific Northwest National Laboratory, Richland, WA, USA

[3] Laboratoire des Sciences du Climat et de l'Environnement, CEA, CNRS, UVSQ/IPSL, Université Paris-Saclay, Orme des Merisiers, Gif-sur-Yvette cedex, France

[4] Division of Geological and Planetary Sciences, California Institute of Technology, Pasadena, USA

[5] Department of Atmospheric Sciences, University of Utah, Salt Lake City, UT, USA

[6] Cooperative Institute for Research in the Atmosphere, Colorado State University, Fort Collins, CO, USA

Contents of this file

Text S1 to S5

Figures S1 to S12

Tables S1 to S3

References

Text S1 More details of the FCSI method

Text S1.1 Background estimation

Two methods were used to calculate the background:

1. 'median': following Schwander et al., (2017) we used the median of the selected sounding as a background value. This method can be seen as conservative as it may overestimate the plume size when the plume width is around (or bigger) half the track length.
2. 'coordFit' : following the idea developed in Ye et al., (2020) we made a planar fit of the track in two step : a first planar fit is done ($(a1,b1,c1) = \mathrm{argmin}_{(a1,b1,c1)}(X_{CO2}(lat,lon)-a1*lat-b1*lon-c1)^2$), the retrieved background ($bckg1 = a1*lat+b1*lon+c1$) is subtracted to the track, we select the soundings under the mean corrected signal plus one standard deviation ($selec = \{lat,lon\}/ (X_{CO2}-bckg1)<(<bckg1>+\sigma_{bckg1})\}$) and make a planar fit on the selected soundings ($(a2,b2,c2) = \mathrm{argmin}_{(a2,b2,c2)}(X_{CO2}(lat,lon)-a2*lat-b2*lon-c2)^2_{(lat,lon)\ in\ selec}$). This second planar interpolation is used as background ($bckg(lon,lat) = a2*lat+b2*lon+c2$) .

Text S1.2 Plume limit detection

Plume limit detection in 2 steps:

1. smoothing (5*6 methods): 5 smoothing methods (using a uniform, a median, a wiener, a gaussian, and a low pass filter) were used on 6 smoothing sizes (from 10 to 25 km wide, with a 3 km step). For the Wiener filter, the noise was set as the mean of the X_{CO2} uncertainty (provided at each sounding in the L2 Lite files) in the track. The detail of the methods can be found in SciPy documentation (https://docs.scipy.org/doc/scipy/reference/ chapter signal for wiener method, ndimage for uniform, Gaussian and median methods, and fftpack for the low pass filter).
2. peak identification (2 methods): maximal peak in the smoothed background subtracted track or closest peak to the estimated effective wind direction – track axis intersection in the smoothed background subtracted track.

All the positive smoothed values surrounding the selected peak are set as a part of the plume.

Text S1.3 Emission zone definition

The emission zone is defined as the zone upwind from the track. To set the limits of the emission zone in the cross-wind direction, we report the plume axis on the plume limits and take the emission within this boundary. The plume axis is set as the axis going from the city center (defined as the maximum if emission in ODIAC) and the middle of the detected plume. Only the ODIAC cells above the median ODIAC cell emission of the targeted zone (corresponding to WRF domain 3) are kept. An illustration can be found in Figure 4. On average, a third of the targeted zone is captured in the emission zone (28% when using all data subsets and 35% when using high-quality tracks).

Text S1.4 Subset selection

We check manually the selected plume and the coherence between the plume axis (plume center – city center axis) and the wind direction to define the criterion of acceptance specific to each date. The criterion is based on two variables: the plume size and the angle between the plume and the estimated effective wind (see Table S1).

Text S1.5 Discussion on the method uncertainty

The error in our methods comes from different steps: the wind evaluation, the background evaluation, the plume detected limits, the emission zone definition, the measurement error, the method representativity error, and the spatial representativity of the used inventory.

Wind angle error: the error related to the wind angle will depend on the angle between the wind and the track normal vector. For an angle of 0° between the track normal vector and the wind, an error of 10° on the wind angle will give an error of 1.5% on the result. For an angle of 60° between the track normal vector and the wind, an error of 10° on the wind angle will give an error of 30% on the result. The error increases with the absolute difference between the wind and the track normal vector and with the wind error.

Wind speed error: the emission error should be linearly related to this error (an error of 10% on the wind modulus will result in an error of 10% on the estimate).

Background calculation error: this error is proportional to the plume size and the wind speed. An error of 0.2 ppm (mean difference between the two retrieved background for the good quality data) on the background for a 30 km plume (classic retrieved plume size) with a 2 m/s wind speed (mean wind in the PBL for the selected dates) and a 1000 hPa dry surface pressure will give an error of approximately 180kg/s on the result, which correspond to 30% of the emission usually detected (600kg/s).

Emission zone error: this error is related to the wind angle error and the plume limits error; we evaluated its spread using 2 masks: a large one (upwind enlarging limits) and the one used in the study. It gives us an error of approximately 10% of variation in the emission.

Method representativity error: our equation is designed for steady state conditions (constant and homogeneous wind, constant emissions) The deviation of the overpass conditions from this steady state is the cause of this error. We applied our method for different pseudo OCO-2 track generated with the WRF simulations a day of highly turning plume (suggesting far from steady state conditions) and found a variation of 30% in the ratio given the track due to this turning shape, whereas the uncertainty is only 5% when the plume has a straight shape (suggesting close from steady state conditions).

Plume detection error: using a pseudo track on a WRF simulation, we made the plume size vary randomly from -15% to +15% (+/- 6km on each side of a 35km plume) to estimate the variation due to error on the plume limits. It gives a spread of 25% of the mean for the emission

111 estimation. Figure S2 shows the standard deviation of the selected subset for each date. Using a
112 subset should reduce this source of uncertainty.
113
114 Measurement error: this error is hopefully unbiased and quantified with the X_{CO2} uncertainty.
115
116 Spatial representativity of the inventory: to evaluate the emission of Lahore, we use a ratio
117 calculated on a fraction of the city (or a fraction of the city and its suburbs). Our estimation relies
118 on the representativity of the inventory. Our subset (by evaluating the emission on different
119 plume limits and thus different emission zone sizes) should reduce this error.
120
121 **Text S2 OCO-2 two-level quality inspection**
122 The OCO-2 X_{CO2} soundings are subject to a two-level quality inspection. The inspection results
123 of each criterion are marked by the variable named "sounding_flag_sel" for the level 1 (L1)
124 product and "xco2_qf_bitflag" for the level 2 (L2) product. The final results are marked by the
125 variable named "xco2_quality_flag" in OCO-2 v9r L2 lite files. The "xco2_quality_flag" is set to
126 0 for high-quality soundings which meet all selection criteria. The "xco2_quality_flag" is set to 1
127 for low-quality soundings that failed to meet one or more criteria.
128
129 We extracted "sounding_flag_sel" from sounding selection (L2Sel) files. The value of
130 "sounding_flag_sel" could be 0, 1, 2, 32. Soundings marked as "sounding_flag_sel = 0" are run
131 through the L2 full-physics retrieval algorithm. Note that "sounding_flag_sel = 0" does not
132 necessarily mean the sounding will show up in L2 data. If it fails to converge, or the code crashes
133 on a sounding in some rare cases, it does not show up in L2 data. Also, soundings over water

that are not in glint mode sometimes run through L2, but they are never included in L2 files. We focus on cities on land in this study. Thus, we exclude the cases that "sounding_flag_sel" does not show up in L2 data. The definitions of selection criteria when "sounding_flag_sel" equaling to 1, 2, 32 are listed as follows:

- flag_1: The cloud cover exceeded max warn level
- flag_2: The cloud cover exceeded warn level cutoff
- flag_32: The sounding has invalid geolocation

The variable "xco2_qf_bitflag" in OCO-2 v9r L2 lite files uses 28 out of the 32 bits of a long integer to report the result of each test. A bit value of 0 means passed, and 1 means failed. If they all pass, the value of this variable will be 0, just as for the normal quality flag variable. Regardless of surface type, the currently-defined 28 bits within this long integer correspond to the following 28 selection criteria (from bit 0 to 27): defined_mode, eof3_3_rel, max_declocking_wco2, max_declocking_sco2, albedo_slope_sco2, rms_rel_wco2, h2o_ratio, co2_ratio, dp_o2a, dp_sco2, co2_grad_del, windspeed, dp_abp, aod_ice, xco2_uncertainty, chi2_wco2, albedo_slope_wco2, surface_type_flipped, altitude_stddev, aod_total, dws, albedo_sco2, rms_rel_sco2, aod_water, ice_height, aod_strataer, aod_oc, aod_seasalt. In OCO-2 Data Product User's Guide (JPL, 2018). Only 24 variables are listed at its Page 25. But definitions of all 28 variables can be found in the user guide. We list definitions of 28 selection criteria when as follows in alphabet sequence:

- albedo_sco2: Over-land retrievals: Surface reflectance at a reference wavelength in band 3 (2.06 μm) in the primary scattering geometry (sun->ground->sensor) derived from the

retrieved BRDF. Over-water retrievals: Retrieved Lambertian albedo at the band 3 reference wavelength.

- aod_seasalt: Retrieved Extinction Optical Depth of sea salt aerosol at 0.755 μm.
- albedo_slope_sco2: Slope of the albedo_sco2 term with respect to wavenumber.
- albedo_slope_wco2: Slope of the albedo_wco2 term with respect to wavenumber.
- altitude_stddev: The standard deviation of the surface elevation in the target field of view, in meters.
- aod_ice: Retrieved Extinction Optical Depth of cloud ice at 0.755 μm.
- aod_oc: Retrieved Extinction Optical Depth of organic carbon at 0.755 μm.
- aod_seasalt: Retrieved Extinction Optical Depth of sea salt aerosol at 0.755 μm.
- aod_strataer: Retrieved Extinction Optical Depth of stratospheric aerosol at 0.755 μm.
- aod_total: Retrieved Extinction Optical Depth of cloud+aerosol at 0.755 μm.
- aod_water: Retrieved Extinction Optical Depth of cloud water at 0.755 μm.
- chi2_wco2: Reduced chi-squared value of the L2 fit residuals for band 2.
- co2_grad_del: Change (between the retrieved profile and the prior profile) of the co2 dry air mole fraction difference from the surface minus that at level 13, measured in ppm. Level 13 is at a pressure P = 0.631579 Psurf. This variable is used in the X_{CO2} bias correction over both land and water surfaces.
- co2_ratio: Contains the ratio of the retrieved CO2 column from the weak Co2 band relative to that from the strong CO2 band. This ratio should be near unity. Significant departure from unity is currently used as a way to flag bad soundings (usually cloud or aerosol-contaminated). This value has also been footprint corrected using

co2_ratio_offset_per_footprint, and further it has been bias corrected to remove a small feature-dependent bias.

- dp_abp: This is the retrieved surface pressure minus the "best-guess" surface pressure from the ECMWF forecast model. This has been adjusted for a clear-sky bias as well as the local surface elevation of the observed footprint. A value of this greater than about 50 hPa absolute value typically indicates cloud or aerosol contamination.
- dp_o2a: The difference psurf – psurf_apriori_sco2, in hPa.
- dp_sco2: The difference psurf – psurf_apriori_sco2, in hPa. This variable is used in the X_{CO2} bias correction over both land and water surfaces.
- dws: Given by aod_dust + aod_water + aod_seasalt. This is used in the X_{CO2} bias correction for soundings over land.
- eof3_3_rel: Relative amplitude of the 3rd EOF in the strong CO2 band.
- h2o_ratio: Contains the ratio of the retrieved H2O column from the weak CO2 band relative to that from the strong CO2 band. This ratio should be near unity. Significant departure from unity is currently used as a way to flag bad soundings (usually cloud or aerosol-contaminated).
- ice_height: Retrieved central pressure of the ice layer, relative to the retrieved surface pressure.
- max_declocking_sco2: An estimate of the absolute value of the clocking error in the strong co2 band (used in the clocking correction algorithm that attempts to correct the L1b radiances for clocking errors). Expressed in percent. Typical values range from 0 to 10%.
- max_declocking_wco2: Same as max_declocking_sco2, but for the weak co2 band.

- rms_rel_sco2: RMS of the L2 fit residuals for band 3, relative to the continuum signal, in percent.
- rms_rel_wco2: RMS of the L2 fit residuals for band 2, relative to the continuum signal, in percent.
- surface_type_flipped: This field is 0 if the surface type is still maintains the same surface type designation as in version 8, and 1 otherwise. As a reminder, the L2 algorithm defines "land" to be >= 80% sounding_land_fraction, and "ocean" (or "water") to be <= 20% for sounding_land_fraction.
- windspeed: Retrieved surface wind speed (in m/s) from the L2 algorithm, over water surfaces only.
- xco2_uncertainty: The posterior uncertainty in X_{CO2} calculated by the L2 algorithm, in ppm. This is generally 30-50% smaller than the true retrieval uncertainty.

Text S3 Main causes for L1/L2 OCO-2 data loss due to quality flag filtering

To investigate the causes behind the OCO-2 L1/L2 data losses, we calculated the failing occurrences of the selection criteria used in quality flags. Figure S6 shows the failing occurrences of 3 criteria in L1 and 27 criteria in the L2 product. The "defined_mode" is not shown in the figure because all soundings pass it over Lahore. See Section Text S2 for the definitions of the selection criteria. Note that a sounding in L2 data a sounding could fail multiple criteria simultaneously, hence the total percentage of L2 quality flags is greater than 100%. Similar to Figure 2, we calculated the percentages in boxes with 25-, 50-, 75-, 100-, and 200-km border-to-center distances around cities. The discrepancy in percentages between selection criteria is significantly greater than the discrepancy between box sizes. For the L1

products, about 70% of the low-quality soundings are caused by cloud-related issues. For the L2 X_{CO2} products, cloud- and aerosol-related criteria cause the greatest loss of data, followed by topography-related criteria.

Text S4 Wind nudging and evaluation

To minimize the X_{CO2} errors caused by model transport error, the analysis nudging in Four-Dimensional Data Assimilation (FDDA) for the outer domain is open (grid_fdda = 1). Figure S7 shows a sample comparison of X_{CO2ff} plume locations between nudged and non-nudged simulations. In the sample case, the X_{CO2ff} plume crossed the OCO-2 track with nudging on while it missed track with nudging off.

To evaluate the uncertainty of WRF-Chem transport, we compared the model wind speed and direction outputs with two datasets, which are NCEP ADP Global Surface Observational Weather Data (NCEP., n.d.) and NCAR Upper Air Database (NCAR n..d). Note that Lahore, Pakistan is growing fast, but still a less-developing area compared to developed countries. The meteorological observation data are still lacking. Only one site in WRF-Chem inner domain can be found in each of the two datasets. The wind speed and direction residuals of WRF-Chem outputs compared to monitor data are shown in Figure S6. The wind speed residual is 2.11 ± 0.38 m/s (1-σ) and the wind direction residual is 10.20 ± 66.04 deg (1-σ). Shahid et al., (2015) evaluated WRF-Chem simulated surface-layer meteorological parameters with a horizontal resolution of 1 degree against the NCEP reanalyzed datasets over Pakistan. The mean bias of U- and V-wind ranged in -0.2 – 0.2 m/s and the normalized mean bias ranged -42.9% to 58.5%. Due to the lack of studies on wind profile evaluation over Lahore or Pakistan, we also compared our

results with WRF studies over Los Angles (LA). Angevine et al. (2012) evaluated WRF at 4 km for California Nexus (CalNex) field campaign over LA using a radar wind profiler operated by the South Coast Air Quality Management District near Los Angeles International Airport (LAX). They found showed 1.1 ± 2.7 m/s bias in wind speed and −2.6 ± 67◦ in wind direction near the surface. Feng et al., 2016 evaluated a set of WRF planetary boundary layer (PBL) schemes performance over LA. They found the biases of the MYNN_UCM scheme are 1.4 ± 2.0 m/s in wind speed and −1.3 ± 20.0◦ in wind direction at the 4 km model resolution.

Text S5 Optimize the OCO-2 quality flag selection criteria

The OCO-2 quality flags are originally designed for global-scale studies. Although we evaluated their effectiveness at the city level in Section 3.5, the valid tracks over Lahore are too few to capture the CO_{2ff} emission trend without relying on the trend of prior (Section 3.6). We tried to optimize the OCO-2 selection criteria based on X_{CO2} residuals between OCO-2 and WRF-Chem. We found that the default thresholds triggering the selection criteria are slightly over-strict (Figure S12). By adequately enlarging the range of thresholds of 8 criteria, we obtained more high-quality soundings (Table S3) but failed to obtain more valid tracks. Further research on more tracks and over more cities is required to confirm if optimization of quality flag selection criteria over cities helps recover valid tracks.

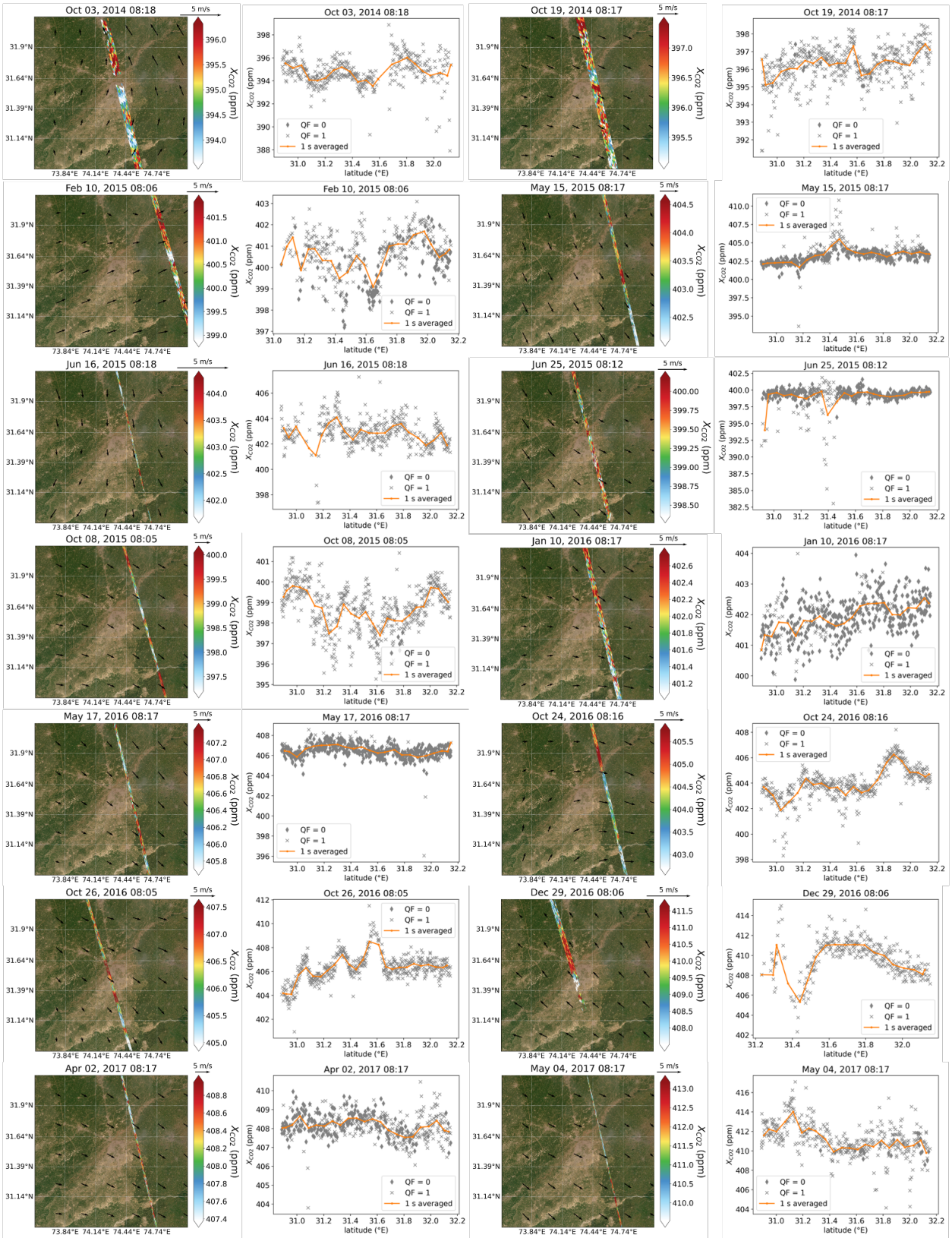
Oct 03, 2014 08:18
Oct 03, 2014 08:18
Oct 19, 2014 08:17
Oct 19, 2014 08:17
Feb 10, 2015 08:06
Feb 10, 2015 08:06
May 15, 2015 08:17
May 15, 2015 08:17
Jun 16, 2015 08:18
Jun 16, 2015 08:18
Jun 25, 2015 08:12
Jun 25, 2015 08:12
Oct 08, 2015 08:05
Oct 08, 2015 08:05
Jan 10, 2016 08:17
Jan 10, 2016 08:17
May 17, 2016 08:17
May 17, 2016 08:17
Oct 24, 2016 08:16
Oct 24, 2016 08:16
Oct 26, 2016 08:05
Oct 26, 2016 08:05
Dec 29, 2016 08:06
Dec 29, 2016 08:06
Apr 02, 2017 08:17
Apr 02, 2017 08:17
May 04, 2017 08:17
May 04, 2017 08:17
5 m/s
X_{CO2} (ppm)
latitude (°E)
QF = 0
QF = 1
1 s averaged
31.9°N
31.64°N
31.39°N
31.14°N
73.84°E 74.14°E 74.44°E 74.74°E

Figure S1 OCO-2 tracks over Lahore. The first and the third columns: The OCO-2 all-data track locations. The colors represent the X_{CO2} mixing ratios. The vectors represent 10-m wind, with the reference vector standing for the wind speed of 5 m/s. The background is the map of Lahore from the ArcGIS REST API service. The second and the fourth columns: The OCO-2 X_{CO2} soundings with quality flags (QF = 0 and QF = 1) and 1-s averaged X_{CO2} along the track latitudes. Note: Tracks filtered with quality flag (QF = 0) on May 15, 2015, June 25, 2015, January 10, 2016, May 17, 2016, April 04, 2017, January 15, 2018, December 01, 2018, February 03, 2019 were selected as high-quality tracks.

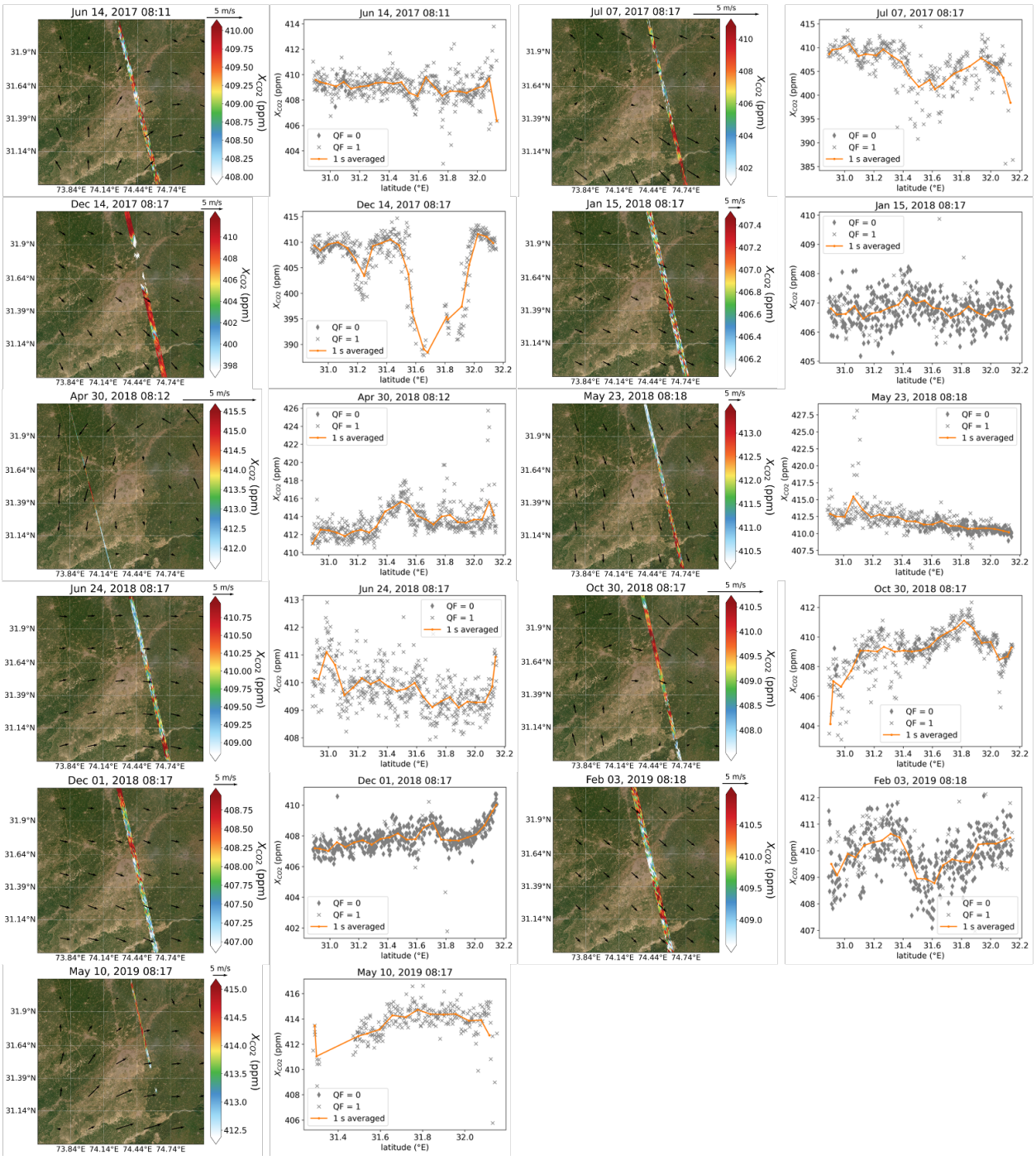

278

279 Figure S1 (Cont.)

280

281

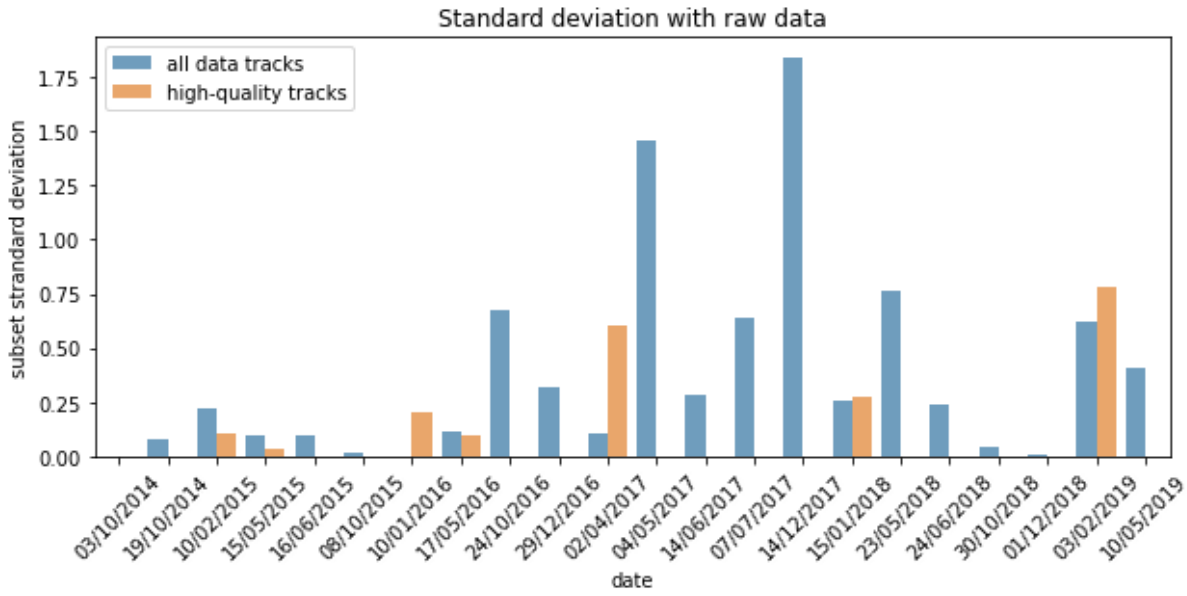

Figure S2 Standard deviation of the selected subset for each date, using all (blue) and only good quality (orange) data from L2LIte_v9r version of OCO2 files. This standard deviation gives an estimation of only a fraction of the estimation uncertainty.

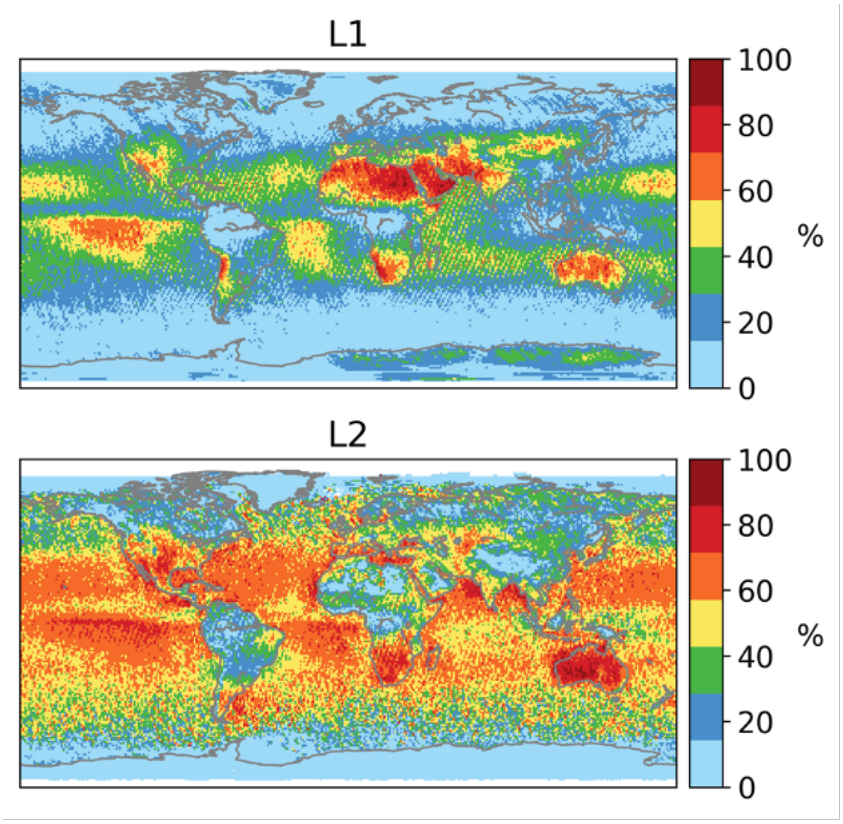

Figure S3 Global 1° x 1° OCO-2 high-quality soundings ratios in L1 and L2 products.

Figure S4 Names and locations of 70 cities.

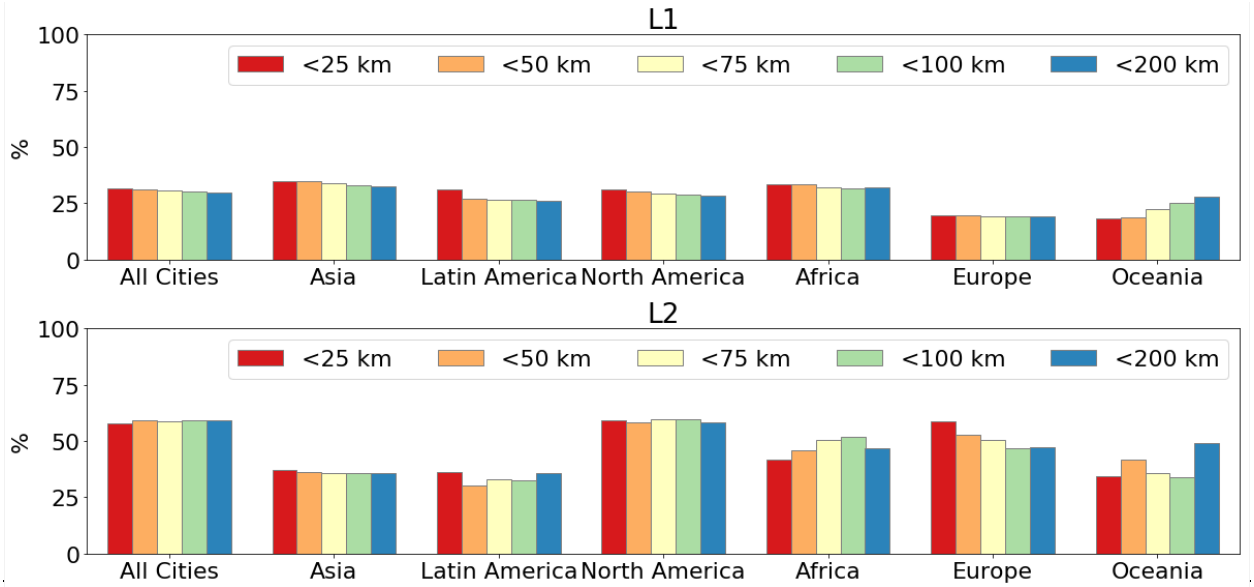

Figure S5 Regional ratios of OCO-2 high-quality soundings in L1 and L2 product over the most populated 70 cities within boxes of 25-, 50-, 75-, 100-, and 200-km border-to-center distance.

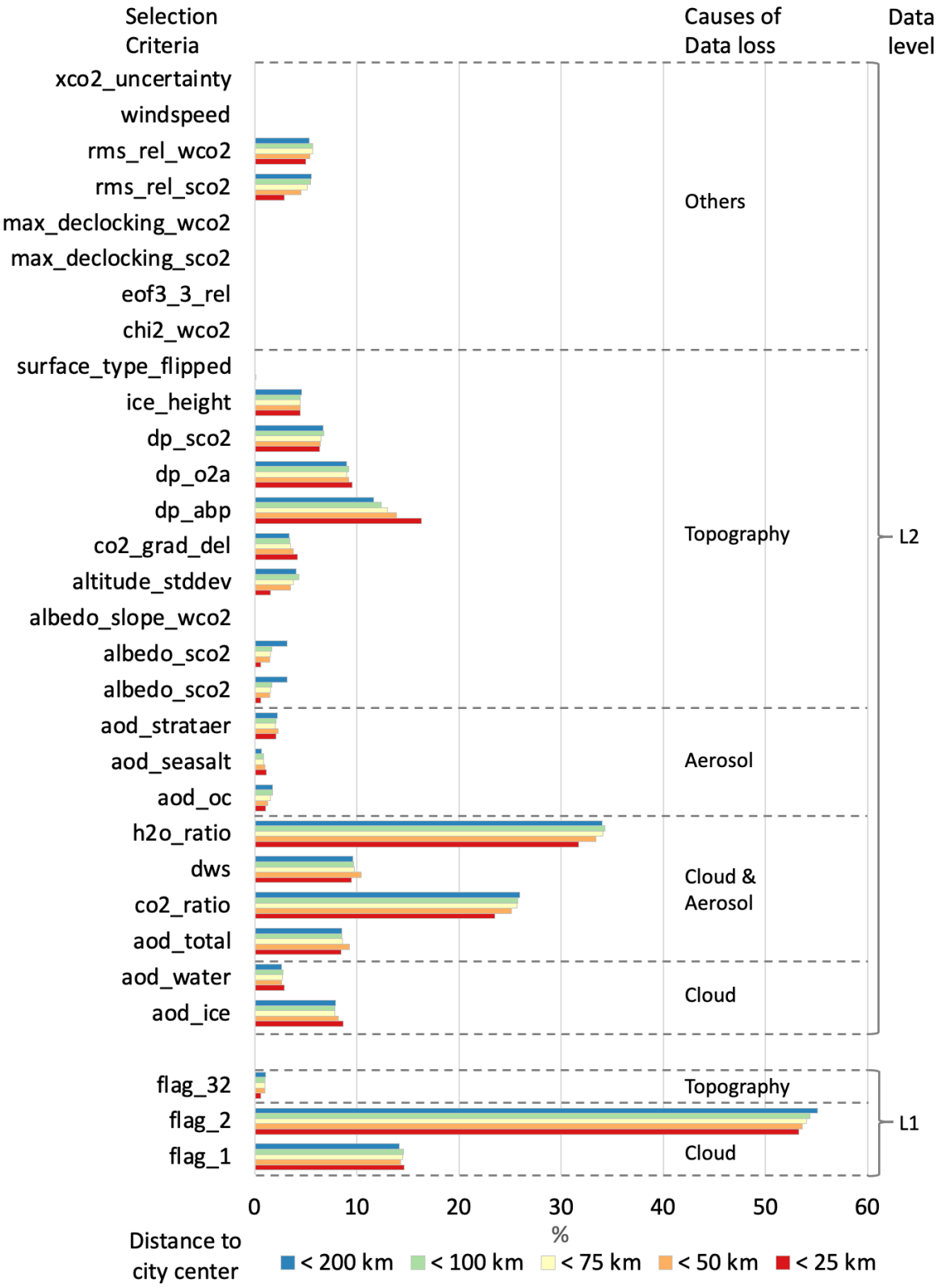

297

298 Figure S6 Percentages of data loss due to each sounding selection criterion over global 70 cities.

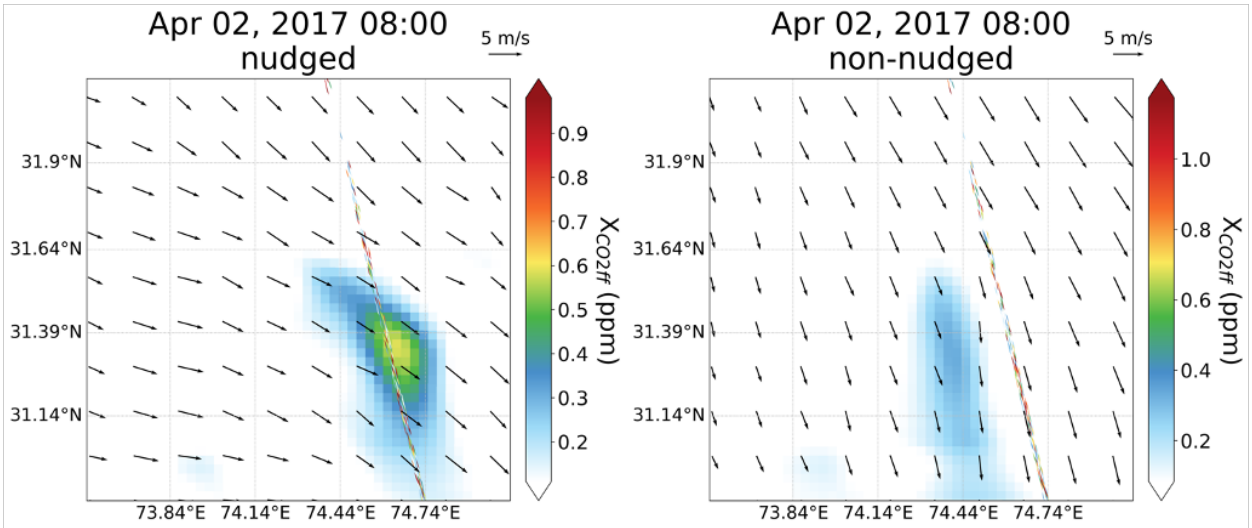

Figure S7 A sample comparison of modeled and observed X_{CO2ff} enhancements between nudged (left) and non-nudged (right) simulations.

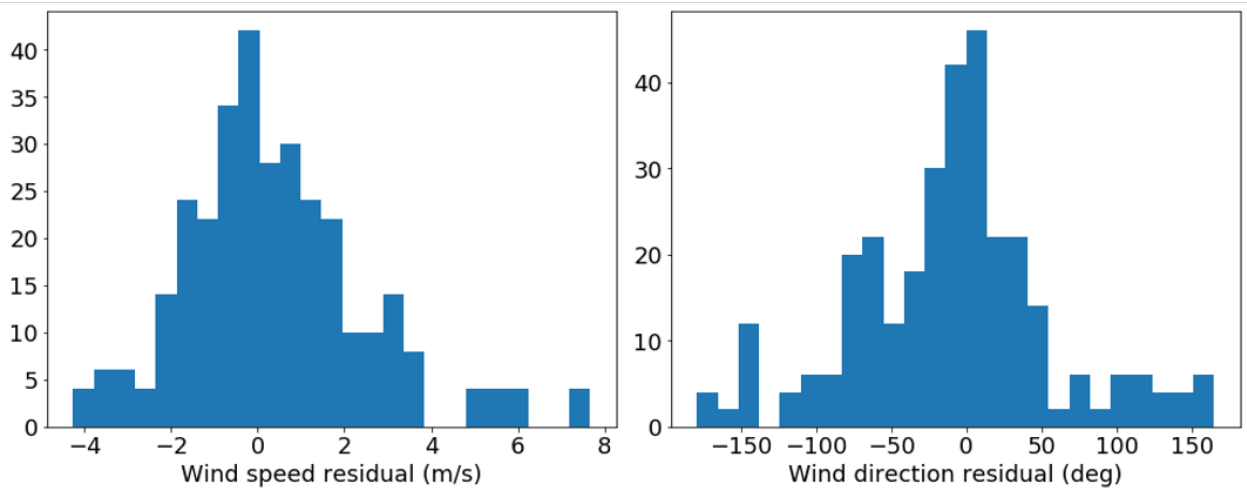

Figure S8 Histograms of wind speed (left) and direction (right) residuals of WRF-Chem outputs compared to monitor data.

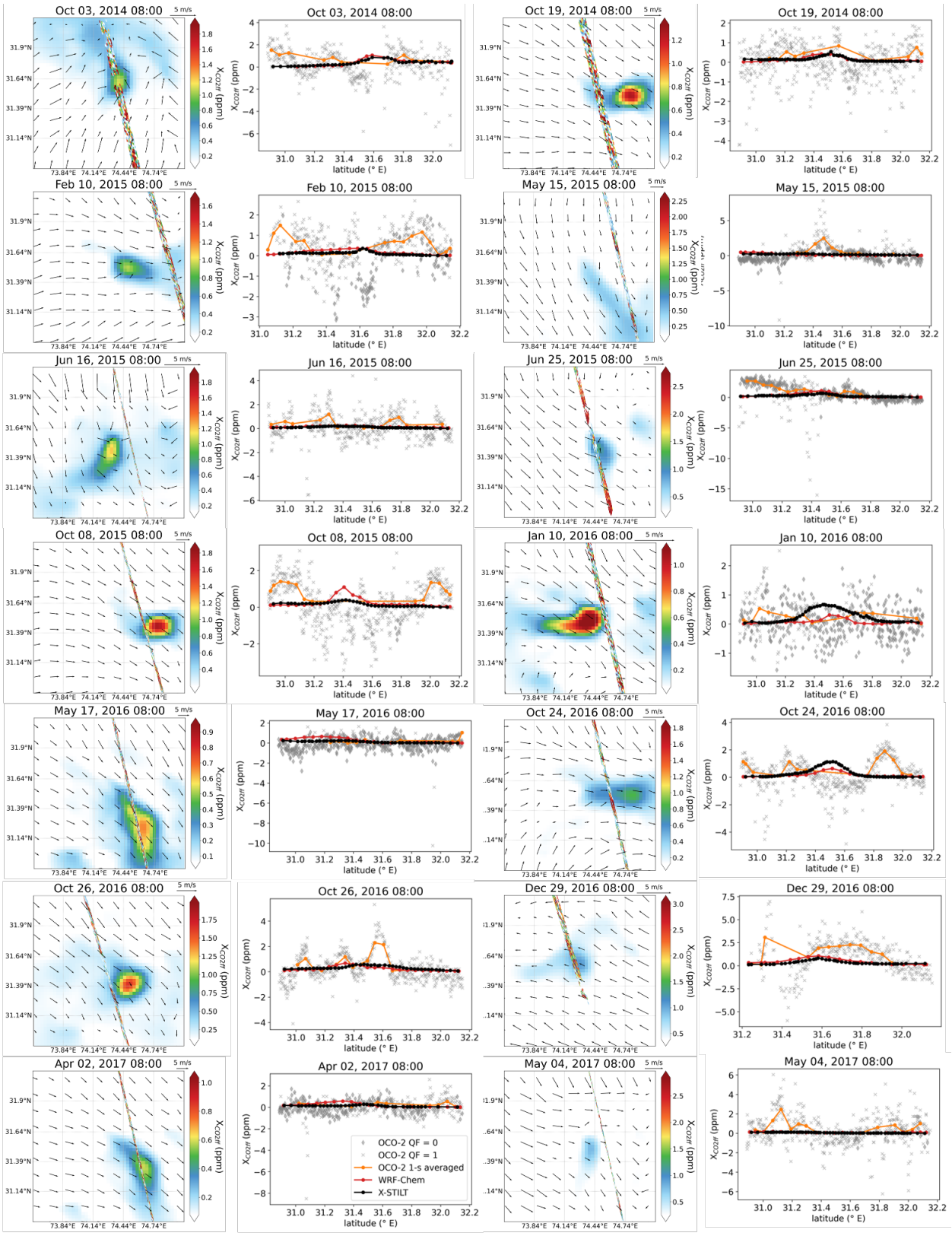
Oct 03, 2014 08:00
Oct 19, 2014 08:00
Feb 10, 2015 08:00
May 15, 2015 08:00
Jun 16, 2015 08:00
Jun 25, 2015 08:00
Oct 08, 2015 08:00
Jan 10, 2016 08:00
May 17, 2016 08:00
Oct 24, 2016 08:00
Oct 26, 2016 08:00
Dec 29, 2016 08:00
Apr 02, 2017 08:00
May 04, 2017 08:00
5 m/s
latitude (° E)
OCO-2 QF = 0
OCO-2 QF = 1
OCO-2 1-s averaged
WRF-Chem
X-STILT

309

Figure S9 Comparison of modeled and observed X_{CO2ff} enhancements by the OCO-2 data for 25 all-data tracks (QF = 0&1) over Lahore. The first and third columns show the simulated X_{CO2ff} by WRF-Chem and the observed X_{CO2ff} obtained from the OCO-2 data (background and biosphere X_{CO2} have been subtracted). The vectors represent 10-m wind from WRF-Chem with the reference vector standing for the wind speed of 5 m/s. The second and fourth columns show the OCO-2 X_{CO2ff} (grey diamond marks represent high-quality (QF = 0) soundings, grey cross marks represent high-quality (QF = 1) soundings, background and biosphere X_{CO2} have been subtracted), 1-s averaged OCO-2 X_{CO2ff} (Orange dotted line), simulated X_{CO2ff} by WRF-Chem (red dotted line) and X-STILT (black dot line).

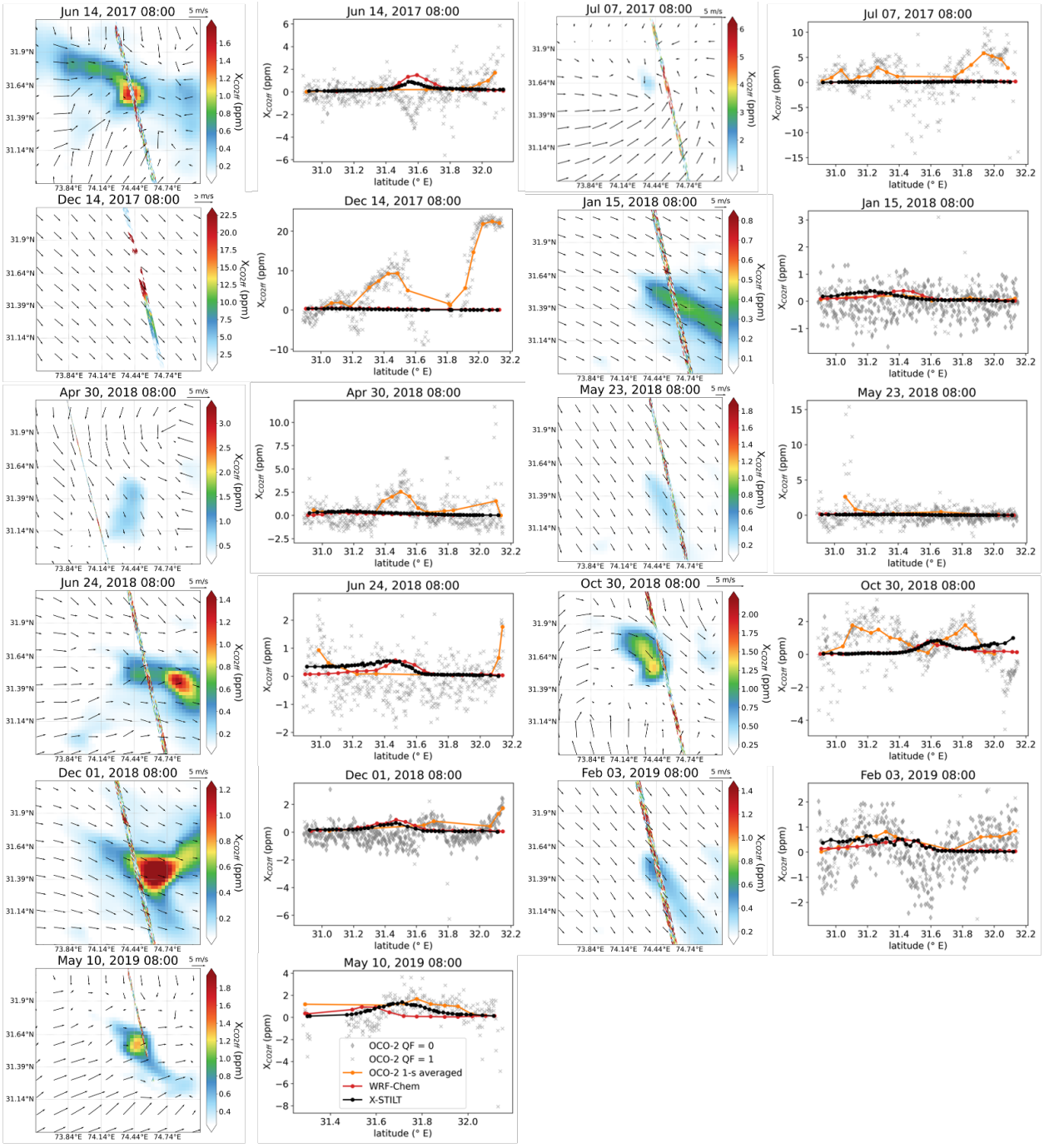

321

322 Figure S9 (Cont.)

323

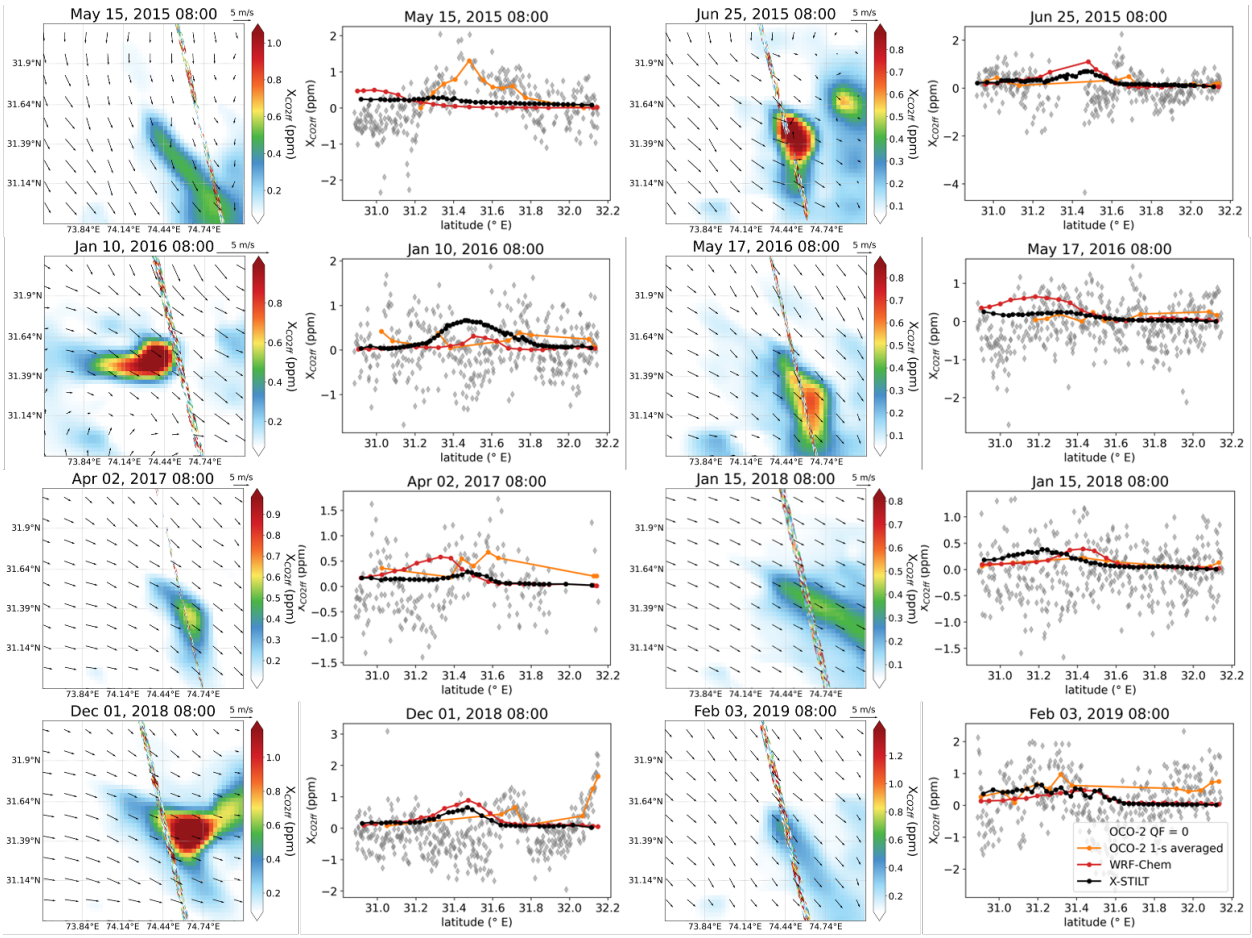

Figure S10 Same as Figure S9 but for 8 high-quality tracks. Low-quality (QF = 1) soundings are filtered out and only keep high-quality (QF = 0) soundings.

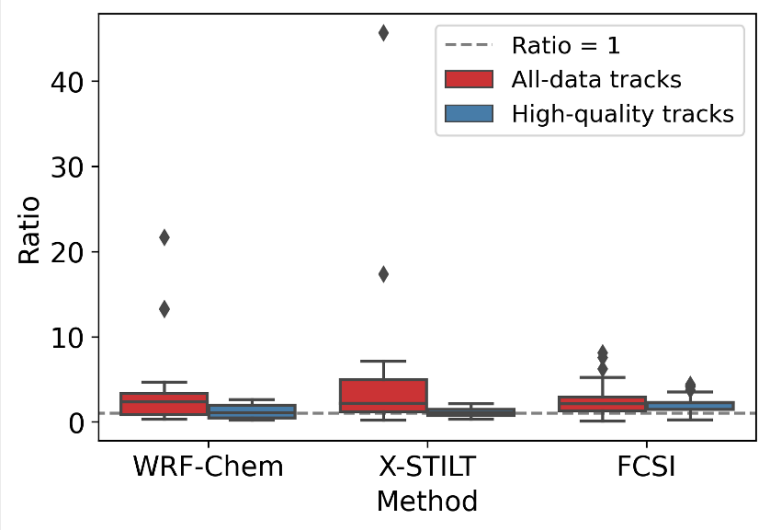

Figure S11 Similar to Figure 5 but show outliers as black diamonds.

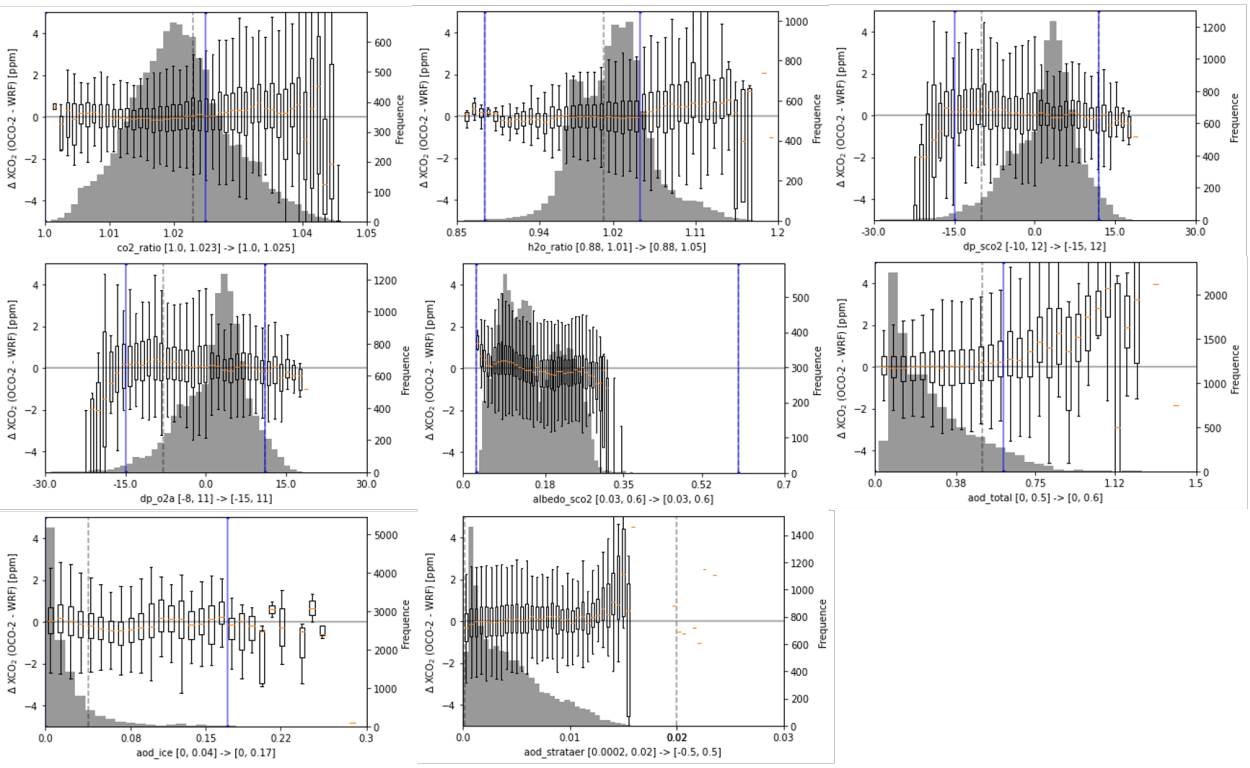

Figure S12 Adjusting thresholds of OCO-2 quality flag selection criteria. The boxes represent the X_{CO2} residuals between OCO-2 and WRF-Chem. For each box, the central line indicates the

median, and the bottom and top edges of the box indicate the 25th and 75th percentiles (q1 and q3), respectively. The outliers are omitted for simplicity. The whiskers extend to the most extreme value that is not an outlier. The grey dashed vertical lines represent the default thresholds of the OCO-2 selection criteria. The blue vertical lines represent the adjusted thresholds based on X_{CO2} residuals. Labels on x-axes show the names of OCO-2 selection criteria and the default and adjusted thresholds trigging the quality flags in the square brackets.

Table S1 Subset selection criteria for each date and data type. θ_{plume}-θ_{wind} is the angle between the plume axis and the wind direction.

	All-data tracks		High-quality tracks	
	Criterion	Subset size after filtering	Criterion	Subset size after filtering
10/03/2014	$\lvert\theta_{plume}-\theta_{wind}\rvert<15°$	1	-	0
19/10/2014	$\lvert\theta_{plume}-\theta_{wind}\rvert<10°$	5	-	0
10/02/2015	$\lvert\theta_{plume}-\theta_{wind}\rvert<7°$	13	$\lvert\theta_{plume}-\theta_{wind}\rvert<30°$	5
15/05/2015	$\lvert\theta_{plume}-\theta_{wind}+35°\rvert<5°$	25	$\lvert\theta_{plume}-\theta_{wind}+35°\rvert<5°$	21
16/06/2015	$\lvert\theta_{plume}-\theta_{wind}\rvert<15°$	22	-	0
25/06/2015	-	0	-	0
08/10/2015	$\lvert\theta_{plume}-\theta_{wind}\rvert<6.5°$ & (plume size)/(track size) >1/10	2	-	
10/01/2016	$\lvert\theta_{plume}-\theta_{wind}\rvert<30°$	1	$\lvert\theta_{plume}-\theta_{wind}\rvert<26°$	3
17/05/2016	$\lvert\theta_{plume}-\theta_{wind}\rvert<7°$	9	$\lvert\theta_{plume}-\theta_{wind}\rvert<7°$	5
24/10/2016	$(\theta_{plume}-\theta_{wind})<0°$	38	-	
26/10/2016	-	0	-	0
29/12/2016	$\lvert\theta_{plume}-\theta_{wind}\rvert<17°$	10	-	0
02/04/2017	$\lvert\theta_{plume}-\theta_{wind}\rvert<10°$	3	$\lvert\theta_{plume}-\theta_{wind}\rvert<5°$	6
04/05/2017	$\lvert\theta_{plume}-\theta_{wind}\rvert<25°$	42	-	0
14/06/2017	$\lvert\theta_{plume}-\theta_{wind}\rvert<36°$	2	-	0
07/07/2017	$\lvert\theta_{plume}-\theta_{wind}\rvert<15°$	22	-	0
14/12/2017	$\lvert\theta_{plume}-\theta_{wind}\rvert<5°$	37	-	0
15/01/2018	$\lvert\theta_{plume}-\theta_{wind}\rvert<2°$	8	$\lvert\theta_{plume}-\theta_{wind}\rvert<4°$	14
30/04/2018	-	0	-	0
23/05/2018	$\lvert\theta_{plume}-\theta_{wind}\rvert<15°$	16	No soundings downwind	0
24/06/2018	$\lvert\theta_{plume}-\theta_{wind}<15°$	8	-	0
30/10/2018	$\lvert\theta_{plume}-\theta_{wind}\rvert<5°$	7	-	0
01/12/2018	$\lvert\theta_{plume}-\theta_{wind}\rvert<10°$	3	$\lvert\theta_{plume}-\theta_{wind}\rvert<7°$	1
03/02/2019	$\lvert\theta_{plume}-\theta_{wind}\rvert<15°$	10	$\lvert\theta_{plume}-\theta_{wind}\rvert<15°$	14
10/05/2019	all	50	-	0

Table S2 Inversion inputs of 8 high-quality tracks over Lahore

Date	Prior total emission (Mt C/year)	Satellite integral X_{CO2ff} (y_o) ± Measurement uncertainty ($\sigma_{measurement}$) (unit: ppm)	Model integral X_{CO2ff} (y_m) ± Transport model uncertainty (σ_{model}) (unit: ppm)
May 15, 2015	8.52E+06	0.37 ± 0.26	0.15 ± 0.23
June 25, 2015	8.55E+06	0.16 ± 0.26	0.44 ± 0.50
January 10, 2016	8.90E+06	0.25 ± 0.22	0.10 ± 0.22
May 17, 2016	9.04E+06	0.17 ± 0.20	0.33 ± 0.21
April 2, 2017	9.57E+06	0.31 ± 0.43	0.26 ± 0.16
January 15, 2018	1.03E+07	0.15 ± 0.28	0.17 ± 0.16
December 1, 2018	1.10E+07	0.07 ± 0.26	0.36 ± 0.66
February 3, 2019	1.06E+07	0.42 ± 0.28	0.24 ± 0.31

363 Table S3 Comparison of high-quality soundings (QF = 0) before and after adjusting the

364 thresholds OCO-2 quality flag selection criteria.

Date	Good soundings (QF = 0)		All soundings (QF = 0&1)
	Before adjusting	After adjusting	
Oct 03, 2014	1	76	411
Oct 19, 2014	19	95	481
Feb 10, 2015	133	284	418
May 15, 2015	338	373	461
Jun 16, 2015	0	243	408
Jun 25, 2015	346	357	449
Oct 08, 2015	8	235	533
Jan 10, 2016	410	456	494
May 17, 2016	434	456	491
Oct 24, 2016	0	79	463
Oct 26, 2016	0	33	498
Dec 29, 2016	0	3	320
Apr 02, 2017	214	385	498
May 04, 2017	24	162	423
Jun 14, 2017	13	166	479
Jul 07, 2017	2	35	347
Dec 14, 2017	18	61	380
Jan 15, 2018	395	459	489
Apr 30, 2018	1	80	535
May 23, 2018	136	209	488
Jun 24, 2018	1	242	487
Oct 30, 2018	45	297	448
Dec 01, 2018	443	478	486
Feb 03, 2019	386	438	487
May 10, 2019	0	16	264

365

References

Angevine, W.M., Eddington, L., Durkee, K., Fairall, C., Bianco, L., Brioude, J., 2012. Meteorological Model Evaluation for CalNex 2010. Mon. Wea. Rev. 140, 3885–3906. https://doi.org/10.1175/MWR-D-12-00042.1

Feng, S., Lauvaux, T., Newman, S., Rao, P., Ahmadov, R., Deng, A., Diaz-Isaac, L.I., Duren, R.M., Fischer, M.L., Gerbig, C., Gurney, K.R., Huang, J., Jeong, S., Li, Z., Miller, C.E., O'Keeffe, D., Patarasuk, R., Sander, S.P., Song, Y., Wong, K.W., Yung, Y.L., 2016. Los Angeles megacity: a high-resolution land–atmosphere modelling system for urban CO2 emissions. Atmospheric Chemistry and Physics (Online) 16. https://doi.org/10.5194/acp-16-9019-2016

JPL, 2018. Orbiting Carbon Observatory–2 (OCO-2) Data Product User's Guide, Operational L1 and L2 Data Versions 8 and Lite File Version [WWW Document]. URL https://docserver.gesdisc.eosdis.nasa.gov/public/project/OCO/OCO2_DUG.V9.pdf Accessed 01 Oct 2020.

NCAR Upper Air Database, 1920-ongoing. Research Data Archive at the National Center for Atmospheric Research, Computational and Information Systems Laboratory. https://rda.ucar.edu/datasets/ds370.1/. Accessed 01 Oct 2020.

NCEP. NCEP ADP Global Upper Air and Surface Weather Observations (PREPBUFR format). Research Data Archive at the National Center for Atmospheric Research, Computational and Information Systems Laboratory. https://doi.org/10.5065/Z83F-N512. Accessed 01 Oct 2020.

Shahid, M.Z., Liao, H., Li, J., Shahid, I., Lodhi, A., Mansha, M., 2015. Seasonal Variations of Aerosols in Pakistan: Contributions of Domestic Anthropogenic Emissions and

Transboundary Transport. Aerosol Air Qual. Res. 15, 1580–1600. https://doi.org/10.4209/aaqr.2014.12.0332

Ye, X., Lauvaux, T., Kort, E.A., Oda, T., Feng, S., Lin, J.C., Yang, E.G., Wu, D., 2020. Constraining Fossil Fuel CO2 Emissions from Urban Area Using OCO-2 Observations of Total Column CO2. Journal of Geophysical Research: Atmospheres 125, e2019JD030528. https://doi.org/10.1029/2019JD030528